STABILITY ANALYSIS OF PIEZOELECTRIC LAMINATED PLATES USING FINITE STRIP METHOD

H. Amoushahi[1], H. Tanzadeh[2]

[1]Department of Civil and Transportation Engineering, University of Isfahan, Isfahan 81746-73441, Iran
Email: h.amoushahi@eng.ui.ac.ir
[1]Department of Civil and Transportation Engineering, University of Isfahan, Isfahan 81746-73441, Iran
Email: h_tanzadeh@trn.ui.ac.ir

Keywords: Stability, Piezoelectric, Laminated Plates, Finite Strip Method

Abstract
A semi analytical finite strip method was developed in present article for buckling of laminated composite plates with piezoelectric layers based on different plate theories. Displacement functions of plate were evaluated using a continuous harmonic function series in the longitudinal direction that satisfies the simply support boundary condition and a piecewise interpolation polynomial in the transverse direction. The analysis conducted based on Reddy's third order shear deformation theory, first order shear deformation theory and classical laminated plate theory. So, considering the strain-displacement relations and stress-strain relations, the standard stiffness and geometry matrices were evaluated using the virtual work principle. The numerical results of buckling of piezoelectric laminated plates based on different plate theories were presented. The effects of different electric conditions, length to thickness ratio and fiber orientation were investigated through the numerical examples.

1. Introduction

Piezoelectric materials are often used to design smart structures in industrial, medical, military and scientific areas. This materials have wide ranging applications that one of the essential features of piezoelectric materials is their ability of transformation between mechanical energy and electric energy. Specifically, when piezoelectric materials are deformed, electric charges are generated, and conversely, the application of an electric field produces mechanical deformations in the structure [1]. In recent years, the increasingly extended application of piezoelectric effects in smart and intelligent structures has led many engineers and researchers to develop more accurate and efficient analysis methods for predicting behaviors of piezoelectric laminated plates [2]. Several research works have been conducted to investigate the stability behaviours of smart composite plates. Panahandeh et al. [3] developed fully coupled electromechanical buckling analysis of active laminated composite thin to thick plates using partial hierarchical Rayleigh Ritz solution. Also they analyzed thermoelastic buckling and active control of thermoelastic buckling for laminated composite plates by piezoelectric actuator and sensor pairs for feedback [4]. Moleiro et al. [5] provided an assessment of layerwise mixed models using least–squares formulation for the coupled electromechanical static analysis of multilayered plates. The functionally graded piezoelectric material is a new type of piezoelectric material in which the electro-elastic properties are considered to vary in thickness direction. Recently, functionally graded piezoelectric structures have attracted great interest among on researchers. Chen et

al. [6] employed the element free Galerkin (EFG) method to analyze buckling of piezoelectric FGM rectangular plates subjected to non-uniformly distributed loads, heat and voltage. The stability analysis of plates made of FGM and subjected to electro-mechanical loading investigated by Jadhav and Bajoria [7].

2. Finite Strip Formulations

The finite strip approach permits the discretization of the rectangular plates in finite longitudinal strips, as shown in Fig. 1.

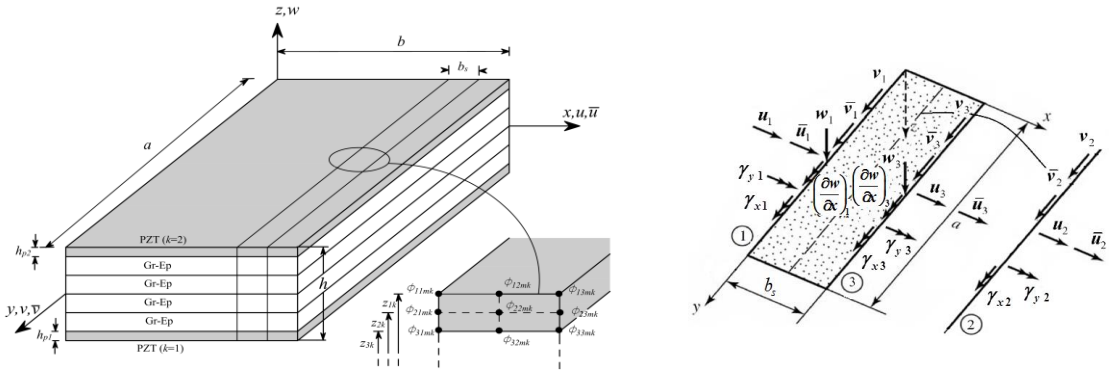

Figure 1. Degrees of freedom in one finite strip: a) Electrical Dofs, b) Mechanical Dofs

The in-plane displacements u_0 and v_0, lateral displacement w_0, rotations of the normal cross sections in x–z (γ_x) and y–z planes (γ_y), and ϕ_k is the electric potential in the kth piezoelectric layer. Therefore these parameters can be taken in the form

$$u_0 = \sum_{m=1}^{r}\sum_{i=1}^{3}\left[N_i(x)\sin(\frac{m\pi y}{a})u_{im} + N_i(x)\cos(\frac{m\pi y}{a})\bar{u}_{im} \right] \quad (1)$$

$$v_0 = \sum_{m=1}^{r}\sum_{i=1}^{3}\left[N_i(x)\cos(\frac{m\pi y}{a})v_{im} + N_i(x)\sin(\frac{m\pi y}{a})\bar{v}_{im} \right] \quad (2)$$

$$w_0 = \sum_{m=1}^{r}\sum_{i=1,3}\left[W_i(x)\sin(\frac{m\pi y}{a})(w_0)_{im} + R_i(x)\sin(\frac{m\pi y}{a})\left(\frac{\partial w_0}{\partial x}\right)_{im} \right] \quad (3)$$

$$\gamma_x = \sum_{m=1}^{r}\sum_{i=1}^{3} N_i(x)\sin(\frac{m\pi y}{a})\gamma_{xim} \quad (4)$$

$$\gamma_y = \sum_{m=1}^{r}\sum_{i=1}^{3} N_i(x)\cos(\frac{m\pi y}{a})\gamma_{yim} \quad (5)$$

$$\phi_k = \sum_{m=1}^{r}\sum_{i=1}^{3}\sum_{p=1}^{3} N_i(x)\sin(\frac{m\pi y}{a})L_{pk}\,\phi_{pkim} \quad (6)$$

The displacement functions are assumed to be polynomials in the transverse direction while, in the longitudinal direction (for out of-plane deformation), characteristics basic functions, simply supported have been used. It should be noted that value of the r in above equations is equal to the number of longitudinal half-wavelengths throughout the plate (number of modes).

$$N_1(x)=1-3\frac{x}{b_s}+2\frac{x^2}{b_s^2},\ N_2(x)=4\frac{x}{b_s}-4\frac{x^2}{b_s^2},\ N_3(x)=2\frac{x^2}{b_s^2}-\frac{x}{b_s} \tag{7}$$

$$W_1(x)=1-3\frac{x^2}{b_s^2}+2\frac{x^3}{b_s^3},\ W_3(x)=3\frac{x^2}{b_s^2}-2\frac{x^3}{b_s^3};\ R_1(x)=-x+2\frac{x^2}{b_s}-\frac{x^3}{b_s^2},\ R_3(x)=\frac{x^2}{b_s}-\frac{x^3}{b_s^2} \tag{8}$$

where b_s is the width of strip. Also, in Eq. (6), $L_{pk}(z)$ for p = 1, 2, 3 are the quadratic interpolation functions in the z direction defined as

$$L_{pk}=\prod_{q=1,\,q\neq p}^{3}\frac{z-z_{qk}}{z_{pk}-z_{qk}} \tag{9}$$

The analysis conducted based on Reddy's third order shear deformation theory (TSDT), first order shear deformation theory (FSDT) and classical laminated plate theory (CLPT). Displacements u, v and w at any point (x, y, z) of the laminate have the following relationships with the midplane displacements:

$$\begin{cases}\mathbf{u}=\mathbf{u_0}+z\,\overline{\mathbf{w}}+\left[\mathbf{F}(z)\right]\overline{\boldsymbol{\gamma}}\\ w=w_0(x,y)\end{cases} \tag{10}$$

in which

$$\mathbf{u}=\begin{Bmatrix}u\\v\end{Bmatrix};\ \mathbf{u_0}=\begin{Bmatrix}u_0\\v_0\end{Bmatrix};\ \overline{\mathbf{w}}=\begin{Bmatrix}\dfrac{\partial w_0}{\partial x}\\[2mm]\dfrac{\partial w_0}{\partial y}\end{Bmatrix};\ \overline{\boldsymbol{\gamma}}=\begin{Bmatrix}\gamma_x\\\gamma_y\end{Bmatrix};\quad \left[\mathbf{F}(z)\right]=\begin{bmatrix}F(z)_{11} & F(z)_{12}\\ F(z)_{21} & F(z)_{22}\end{bmatrix} \tag{11}$$

In Eq. (11), $\left[\mathbf{F}(z)\right]$ for various plate theories can be defined as

$$\begin{cases}F(z)_{11}=F(z)_{22}=z(1-\dfrac{4z^2}{3h^2});\quad F(z)_{21}=F(z)_{12}=0 & \textit{for TSDT}\\ F(z)_{11}=F(z)_{22}=z;\quad F(z)_{21}=F(z)_{12}=0 & \textit{for FSDT}\\ F(z)_{11}=F(z)_{22}=0;\quad F(z)_{21}=F(z)_{12}=0 & \textit{for CLPT}\end{cases} \tag{12}$$

The generalized displacements have the following linear relationships with the generalized strains:

$$\boldsymbol{\varepsilon}=\begin{Bmatrix}\varepsilon_x & \varepsilon_y & \gamma_{xy}\end{Bmatrix}^{\mathrm{T}}=\begin{Bmatrix}\dfrac{\partial u}{\partial x} & \dfrac{\partial v}{\partial y} & \dfrac{\partial u}{\partial y}+\dfrac{\partial v}{\partial x}\end{Bmatrix}^{\mathrm{T}} \tag{13}$$

$$\boldsymbol{\gamma}=\begin{Bmatrix}\gamma_{yz} & \gamma_{xz}\end{Bmatrix}^{\mathrm{T}}=\begin{Bmatrix}\dfrac{\partial v}{\partial z}+\dfrac{\partial w}{\partial y} & \dfrac{\partial u}{\partial z}+\dfrac{\partial w}{\partial x}\end{Bmatrix}^{\mathrm{T}} \tag{14}$$

$$\mathbf{E}=\begin{Bmatrix}-E_x & -E_y & -E_z\end{Bmatrix}^{\mathrm{T}}=\begin{Bmatrix}\dfrac{\partial \phi}{\partial x} & \dfrac{\partial \phi}{\partial y} & \dfrac{\partial \phi}{\partial z}\end{Bmatrix}^{\mathrm{T}} \tag{15}$$

in which **ε**, **γ**, **E,** are the bending strain, shear strain, and electric field vectors, respectively.

The stress–strain constitutive law for the material of each layer of piezoelectric laminate, considering linear piezoelectricity can be given in matrix notation as

$$\begin{Bmatrix}\boldsymbol{\sigma}^{(k)}\\ \boldsymbol{\tau}^{(k)}\\ \mathbf{D}^{(k)}\end{Bmatrix}_{8\times1}=\begin{bmatrix}\bar{\mathbf{Q}}_{\mathbf{b}}^{(k)} & \mathbf{0} & \bar{\mathbf{e}}_{\mathbf{b}}^{(k)}\\ \mathbf{0} & \bar{\mathbf{Q}}_{\mathbf{s}}^{(k)} & \bar{\mathbf{e}}_{\mathbf{s}}^{(k)}\\ \bar{\mathbf{e}}_{\mathbf{b}}^{(k)^{\mathrm{T}}} & \bar{\mathbf{e}}_{\mathbf{s}}^{(k)^{\mathrm{T}}} & \boldsymbol{\eta}^{(k)}\end{bmatrix}_{8\times8}\begin{Bmatrix}\boldsymbol{\varepsilon}\\ \boldsymbol{\gamma}\\ \mathbf{E}\end{Bmatrix}_{8\times1} \tag{16}$$

in which $\boldsymbol{\sigma}^{(k)}$, $\boldsymbol{\tau}^{(k)}$ and $\mathbf{D}^{(k)}$ are bending stress, shear stress and the electric displacement vectors, respectively, that could be defined as

$$\boldsymbol{\sigma}^{(k)} = \left\langle \sigma_x \quad \sigma_y \quad \tau_{xy} \right\rangle^{\mathrm{T}} \tag{17}$$

$$\boldsymbol{\tau}^{(k)} = \left\langle \tau_{yz} \quad \tau_{zx} \right\rangle^{\mathrm{T}} \tag{18}$$

$$\mathbf{D}^{(k)} = \left\langle D_x \quad D_y \quad D_z \right\rangle^{\mathrm{T}} \tag{19}$$

Also, $\bar{\mathbf{Q}}_{\mathbf{b}}^{(k)}$ and $\bar{\mathbf{Q}}_{\mathbf{s}}^{(k)}$ are the plane stress reduced stiffness matrix for in-plane normal/shear and out-of-plane shear, respectively. $\bar{\mathbf{e}}_{\mathbf{b}}^{(k)}$ and $\bar{\mathbf{e}}_{\mathbf{s}}^{(k)}$ are the bending and shear matrices of reduced piezoelectric coefficients, respectively. $\boldsymbol{\eta}^{(k)}$ is the electric permittivity matrix, that these parameters are defined in Ref. [8].

In present study, the standard finite element procedure, based on virtual work is used to derive stiffness and geometric matrices. The finite element formulation can be obtained from equation

$$\delta W_{int}^{e} = \delta W_{ext}^{N} \tag{20}$$

in which δ is the variational operator, W_{int}^{e} is the internal work and δW_{ext}^{N} is external work for buckling analysis, defined by equations

$$W_{\mathrm{int}}^{e} = \frac{1}{2}\int \left(\boldsymbol{\varepsilon}^{\mathrm{T}}\boldsymbol{\sigma} + \boldsymbol{\gamma}^{\mathrm{T}}\boldsymbol{\tau} + \mathbf{E}^{\mathrm{T}}\mathbf{D} \right) dV \tag{21}$$

$$\mathrm{W}_{ext}^{N} = \mathrm{W}_{ext}^{u} + \mathrm{W}_{ext}^{v} + \mathrm{W}_{ext}^{w} = \frac{1}{2}\int \mathbf{G}_{\mathbf{u}}^{\mathrm{T}}\boldsymbol{\sigma}_{\mathbf{0}}\mathbf{G}_{\mathbf{u}}\, dV + \frac{1}{2}\int \mathbf{G}_{\mathbf{v}}^{\mathrm{T}}\boldsymbol{\sigma}_{\mathbf{0}}\mathbf{G}_{\mathbf{v}}\, dV + \frac{1}{2}\int \mathbf{G}_{\mathbf{w}}^{\mathrm{T}}\boldsymbol{\sigma}_{\mathbf{0}}\mathbf{G}_{\mathbf{w}}\, dV \tag{22}$$

$\boldsymbol{\sigma}_{\mathbf{0}}$ is the in-plane force per unit length matrix expressed as

$$\boldsymbol{\sigma}_{\mathbf{0}} = \frac{1}{h}\begin{bmatrix} n_x & n_{xy} \\ n_{xy} & n_y \end{bmatrix} \tag{23}$$

in which, n_x and n_y are in-plane force per unit length in x and y direction and n_{xy} is in-plane shear force per unit length, where V denote the volume of the strip. In addition $\mathbf{G}_{\mathbf{u}}$, $\mathbf{G}_{\mathbf{v}}$ and $\mathbf{G}_{\mathbf{w}}$ could be defined as

$$\mathbf{G}_{\mathbf{u}} = \left\{ \frac{\partial u}{\partial x} \quad \frac{\partial u}{\partial y} \right\}^{T}; \quad \mathbf{G}_{\mathbf{v}} = \left\{ \frac{\partial v}{\partial x} \quad \frac{\partial v}{\partial y} \right\}^{T}; \quad \mathbf{G}_{\mathbf{w}} = \left\{ \frac{\partial w}{\partial x} \quad \frac{\partial w}{\partial y} \right\}^{T} \tag{24}$$

By substituting Eqs. (1)-(6), in Eqs. (13)-(15) and Eq. (25), and finally in Eqs. (21) and (22), the Eq. (20) can be rewritten

$$\delta W_{int}^{e} = \delta \boldsymbol{\Delta}^{T}\mathbf{K}\boldsymbol{\Delta}; \quad \mathbf{K} = \mathbf{K}_{\mathbf{b}} + \mathbf{K}_{\mathbf{s}} + \mathbf{K}_{\mathbf{E}_1} + \mathbf{K}_{\mathbf{E}_2} \tag{25}$$

$$\delta W_{ext}^{N} = \delta \boldsymbol{\Delta}^{T}\mathbf{K}_{\mathbf{g}}\boldsymbol{\Delta}; \quad \mathbf{K}_{\mathbf{g}} = \mathbf{K}_{\mathbf{gu}} + \mathbf{K}_{\mathbf{gv}} + \mathbf{K}_{\mathbf{gw}} \tag{26}$$

in which δΔ is the virtual displacement vector and **K**, **Kg** and **M** are standard stiffness and geometric stiffness, respectively, that could be described by following equations.

$$\begin{aligned}
\mathbf{K}_{\mathbf{b}} &= \int_V (\mathbf{B}^{\mathbf{b}})^{\mathrm{T}} \bar{\mathbf{Q}}_{\mathbf{b}} \mathbf{B}^{\mathbf{b}} dV + \int_{V_{p1}} (\mathbf{B}^{\mathbf{b}})^{\mathrm{T}} \bar{\mathbf{e}}_{\mathbf{b}} \mathbf{B}^{\mathbf{p1}} dV + \int_{V_{p2}} (\mathbf{B}^{\mathbf{b}})^{\mathrm{T}} \bar{\mathbf{e}}_{\mathbf{b}} \mathbf{B}^{\mathbf{p2}} dV \\
\mathbf{K}_{\mathbf{s}} &= \int_V (\mathbf{B}^{\mathbf{s}})^{\mathrm{T}} \bar{\mathbf{Q}}_{\mathbf{s}} \mathbf{B}^{\mathbf{s}} dV + \int_{V_{p1}} (\mathbf{B}^{\mathbf{s}})^{\mathrm{T}} \bar{\mathbf{e}}_{\mathbf{s}} \mathbf{B}^{\mathbf{p1}} dV + \int_{V_{p2}} (\mathbf{B}^{\mathbf{s}})^{\mathrm{T}} \bar{\mathbf{e}}_{\mathbf{s}} \mathbf{B}^{\mathbf{p2}} dV \\
\mathbf{K}_{\mathbf{E}_1} &= \int_{V_{p1}} (\mathbf{B}^{\mathbf{p1}})^{\mathrm{T}} \bar{\mathbf{e}}_{\mathbf{b}}^{\mathrm{T}} \mathbf{B}^{\mathbf{b}} dV + \int_{V_{p1}} (\mathbf{B}^{\mathbf{p1}})^{\mathrm{T}} \bar{\mathbf{e}}_{\mathbf{s}}^{\mathrm{T}} \mathbf{B}^{\mathbf{s}} dV + \int_{V_{p1}} (\mathbf{B}^{\mathbf{p1}})^{\mathrm{T}} \boldsymbol{\eta} \mathbf{B}^{\mathbf{p1}} dV \\
\mathbf{K}_{\mathbf{E}_2} &= \int_{V_{p2}} (\mathbf{B}^{\mathbf{p2}})^{\mathrm{T}} \bar{\mathbf{e}}_{\mathbf{b}}^{\mathrm{T}} \mathbf{B}^{\mathbf{b}} dV + \int_{V_{p2}} (\mathbf{B}^{\mathbf{p2}})^{\mathrm{T}} \bar{\mathbf{e}}_{\mathbf{s}}^{\mathrm{T}} \mathbf{B}^{\mathbf{s}} dV + \int_{V_{p2}} (\mathbf{B}^{\mathbf{p2}})^{\mathrm{T}} \boldsymbol{\eta} \mathbf{B}^{\mathbf{p2}} dV
\end{aligned} \tag{27}$$

$$\mathbf{K}_{gu} = \int_V (\mathbf{B}^u)^T \boldsymbol{\sigma}_0 \mathbf{B}^u dV$$
$$\mathbf{K}_{gv} = \int_V (\mathbf{B}^v)^T \boldsymbol{\sigma}_0 \mathbf{B}^v dV \quad (28)$$
$$\mathbf{K}_{gw} = \int_V (\mathbf{B}^w)^T \boldsymbol{\sigma}_0 \mathbf{B}^w dV$$

Finally, according to satisfy the Eq. (20) for any virtual displacement vector of $(\delta\Delta)^T$, the finite strip buckling formulations was obtained as

$$\left(\mathbf{K} - \lambda \mathbf{K}_g\right)\boldsymbol{\Delta} = 0 \quad (29)$$

where, λ and is the critical load factor of the laminate plate.

3. Results

In the following, the stability formulations for analysis of piezoelectric laminated composite plates based on various plate theories extracted by the virtual work principle and using the finite strip method. In order to verify the proposed analysis and finite strip method, the present results are compared with other references. In present section a piezoelectric laminate plate with simply supported on four edges is considered. Each piezoelectric layer has thickness of 0.1*h* and other elastic layers have equal thickness, unless otherwise noted. The plate is modeled by ten finite strips and one mode (r = 1) in all cases. The numerical results of buckling of piezoelectric laminated plates exposed to in-plane force and strain, and electrical potential were presented. The effects of electrical conditions, length to thickness ratio and fiber orientation were investigated through numerical examples as shown in Tables 1-4 and Fig. 2. The material properties and electrical conditions are described in Refs. [8, 10]. It could be noted that, "Open-Circuit-C" is defined Open-circuit when inner electrodes are continuous and "Open-Circuit-N" is defined Open-circuit when there is no inner electrode.

3.1. Buckling load under in-plane strain and electrical potential

For electrical buckling, the inner surface of each PZT layer is grounded, whereas the uniform electrical potentials ϕ and $-\phi$ are applied to the outer surfaces of the two PZT layers with immovable edges (ε_x = εy = γ_{xy} = 0). In present sub–section, the critical potential and buckling load under in-plane strain were calculated for different aspect to thickness ratio and the results were shown in Tables 1 and 2. The results were compared with other references for verifying the accuracy of them.

Table 1. Normalized uniaxial strain and electrical potential of square [p/0°/90°/90°/0°/p] laminate based on TSDT with Gr-Ep (E_1=181GPa) and PZT-5A for elastic and piezoelectric layers, respectively.

	$\bar{\varepsilon}_{cr} = \varepsilon_{xcr}\, a^2/h^2$				$\bar{\phi}_{cr} = \phi_{cr}\, d_{33p}\, a^2/h^2$	
	Close Circuit		Open Circuit-N		$(\varepsilon_x^0 = \varepsilon_y^0 = \gamma_{xy}^0 = 0)$	
a/h	Present study	Ref. [2]	Present study	Ref. [2]	Present study	Ref. [2]
5	1.0162	0.9053	1.0603	0.9046	0.5671	0.5218
10	1.6463	1.5797	1.8064	1.6291	0.9264	0.8906
20	1.9713	1.9446	2.1839	2.0305	1.1206	1.1055
100	2.1071	2.1073	2.3459	2.2123	1.2034	1.2025

Table 2. Normalized uniaxial buckling strain of square [p/0°/90°/90°/0°/p] laminate for "Close Circuit-N" electrical condition (Gr-Ep (E_1=181GPa) and PZT-5A).

		$\bar{\varepsilon}_{cr} = \varepsilon_{xcr}\, a^2 / h^2$					
		Present study	Ref. [8]	Present study	Ref. [8]	Present study	Ref. [8]
Theory	*a*/*h*	5 (0.9295)*		10 (1.5977)*		20 (1.9515)*	
TSDT		1.0162	1.0169	1.6463	1.6467	1.9713	1.9714
FSDT		1.2488	1.2480	1.7927	1.7920	2.0229	2.0219
CLPT		1.9457	1.9448	2.0646	2.0689	2.1215	2.1024

* Exact 3D in Ref. [9]

3.2. Buckling load under in-plane force and electrical potential

The critical uniaxial buckling load and critical potential of simply supported square laminates based on Reddy's higher order theory was compared with other references in Tables 3 and 4. the critical potential and buckling load under in-plane force were calculated for different aspect to thickness ratio , different electrical conditions and different orientation of laminates.
As is evident the results have a good agreement with those obtained in the literature. Table 3 show that the piezoelectric laminate with the Close Circuit conditions has only slightly different than the proportional elastic solutions on critical buckling forces and but with Open Circuit conditions has significantly effect than the Close Circuit conditions and also elastic solutions.

Table 3. Normalized buckling load of square piezoelectric laminated plates based on TSDT (Gr-Ep (E_1=181GPa) and PZT-5A).

a/*h*	Lay-ups	Method	$\bar{N} = N_{xcr}\, a^2 / E_{2,Gr-Ep}\, h^3$			
			Elastic solution	Close-Circuit	Open-circuit-C	Open-circuit-N
10	[p/0°/90°/90°/0°/p]	Present study	15.7004	15.7090	16.8895	17.2341
		Ref. [8]	15.64	15.65	16.58	17.10
		Ref. [3]	-	15.8703	16.9848	-
	[p/45°/-45°/45°/-45°/p]	Present study	18.7823	18.7896	19.8896	20.2203
		Ref. [8]	18.81	18.82	19.68	20.19
20	[p/0°/90°/90°/0°/p]	Present study	18.7576	18.7668	20.3381	20.7923
		Ref. [8]	18.73	18.74	20.01	20.71
		Ref. [3]	-	18.8260	20.3210	-
	[p/45°/-45°/45°/-45°/p]	Present study	22.7894	22.8019	24.3289	24.7870
		Ref. [8]	22.77	22.81	24.05	24.77
100	[p/0°/90°/90°/0°/p]	Present study	20.0442	20.0537	21.8058	22.3102
		Ref. [8]	20.04	20.06	21.48	22.26
		Ref. [3]	-	20.0474	21.7151	-
	[p/45°/-45°/45°/-45°/p]	Present study	24.4859	24.4951	26.2312	26.7501
		Ref. [8]	24.49	24.5	25.91	26.73

Table 4. Critical buckling load (kN/m) and critical electrical potential (V) of [p/0°/90°/90°/0°/p] square laminate with a = 200mm, h = 1mm, $h_{p1} = h_{p2}$ = 0.25mm based on TSDT (Gr-Ep (E_1=181GPa) and PZT-5).

Method	Critical buckling load (kN/m)			Critical potential
	Close Circuit	Open Circuit-N	Elastic solution	
Present study	5.4154	6.6367	5.3693	68.2822
Ref. [10]	5.413	6.590	5.369	68.45
Ref. [11]	5.33	7.22	5.37	68.8

3.3. Interaction curve of biaxial in-plane loading

The effect of biaxial in-plane force on the buckling of square thick laminated piezoelectric plates is investigated using the finite strip method. For this purpose, the square thick piezoelectric laminated composite plate with simply supported edges is considered subjected to biaxial in-plane loading under different electric boundary conditions. The interaction curves was shown in Fig. 2 for [p/45°/-45°/45°/-45°/p] laminate. Fig. 2 was drawn for different length to thickness ratio a/h = 10, 20 and 100. In all curves, the piezoelectric layers made of PZT-5A with thickness of 0.1h are located on top and bottom surfaces, whereas, each elastic layers has the thickness of 0.2h and made of Graphite-Epoxy with (E_1=181 GPa). The results show the linear behavior for all electric boundary conditions and length to thickness ratio.

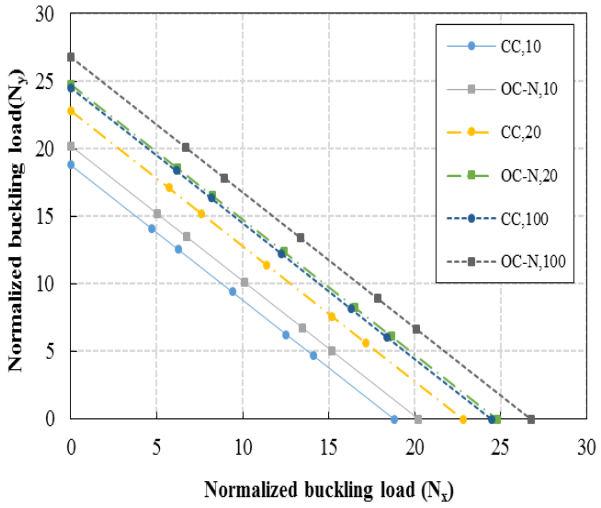

Figure 2. Interaction curve of biaxial in-plane forces loading [p/45°/-45°/45°/-45°/p] on square piezoelectric laminate for different electric boundary conditions and aspect to thickness ratio based on TSDT (Gr-Ep (E_1=181GPa) and PZT-5A).

4. Conclusions

In the present study, the finite strip formulation was developed for stability analysis of piezoelectric symmetric cross–ply and antisymmetric angle-ply laminates based on various plate theories. The finite

strip procedure based on the virtual work principle was used to derive the stiffness and geometric matrices. The accuracy of the proposed method was verified and was in a reasonable agreement by comparing its numerical predictions with published data. Numerical examples show that the piezoelectric laminate with the Close Circuit conditions has only slightly different than the proportional elastic solutions on critical buckling forces but with Open Circuit conditions has significantly effect than the Close Circuit conditions and also elastic solutions. Also the results show the linear behavior for all electric boundary conditions and length to thickness ratio for biaxial loading.

References

[1] P. Phung-Van, L. De Lorenzis, C. H. Thai, M. Abdel-Wahab, and H. Nguyen-Xuan. Analysis of laminated composite plates integrated with piezoelectric sensors and actuators using higher-order shear deformation theory and isogeometric finite elements. *Computational Materials Science,* 96: 495–505, 2015.

[2] G. Akhras, and W. Li. Three-dimensional stability analysis of piezoelectric antisym-490 metric angle-ply laminates using finite layer method. *Journal of Intelligent Material Systems and Structures*, 21:719-727, 2010.

[3] D. Panahandeh-Shahraki, H. R. Mirdamadi, and O. Vaseghi. Fully coupled electro-mechanical buckling analysis of active laminated composite plates considering stored voltage in actuators. *Composite Structures*, 118:94-105, 2014.

[4] D. Panahandeh-Shahraki, H. R. Mirdamadi, and O. Vaseghi. Thermoelastic buckling analysis of laminated piezoelectric composite plates. *International Journal of Mechanics and Materials in Design*, 11:371-385, 2015.

[5] F. Moleiro, C. M. Soares, C. M. Soares, and J. Reddy. Layerwise mixed models for analysis of multilayered piezoelectric composite plates using least-squares formulation. *Composite Structures*, 119:134-149, 2015.

[6] X. Chen, Z. Zhao, and K. Liew, Efg based stability analysis of piezoelectric fgm plates subjected to electricity, heat and non-uniformly distributed loads. *WIT transactions on modelling and simulation*, 39:307-317, 2005.

[7] P. Jadhav, and K. Bajoria. Stability analysis of piezoelectric fgm plate subjected to electro mechanical loading using finite element method. *Int. J. Appl. Sci. Eng*, 11:375-391, 2013.

[8] G. Akhras, and W. Li. Stability and free vibration analysis of thick piezoelectric composite plates using spline finite strip method. *International Journal of Mechanical Sciences*, 53:575-584, 2011.

[9] S. Kapuria, and G. Achary. Exact 3-d piezoelasticity solution for buckling of hybrid cross-ply plates using transfer matrices. *Acta mechanica* 170: 25-45, 2004.

[10] G. Akhras, and W. Li. Three-dimensional static, vibration and stability analysis of piezoelectric composite plates using a finite layer method. *Smart materials and structures*, 16:561-569, 2007.

[11] D. Varelis, and D. A. Saravanos. Nonlinear coupled mechanics and initial buckling of composite plates with piezoelectric actuators and sensors. *Smart materials and structures*, 11:330-336, 2002.